THE JOURNAL OF PHYSICAL CHEMISTRY C
A JOURNAL OF THE AMERICAN CHEMICAL SOCIETY

pubs.acs.org/JPCC

Article

Structure–Reactivity Relationship in the High-Pressure Formation of Double-Core Carbon Nanothreads from Azobenzene Crystal

Sebastiano Romi, Samuele Fanetti,* Frederico Alabarse, and Roberto Bini

Cite This: *J. Phys. Chem. C* 2021, 125, 17174–17182

Read Online

ACCESS | Metrics & More | Article Recommendations | Supporting Information

ABSTRACT: Saturated carbon nanothreads are one of the most attractive new materials produced under high pressure in the last years. Nanothreads can be considered as a monodimensional diamond; in fact, they preserve some of the mechanical properties of the diamond itself, like stiffness, but their intrinsic flexibility makes them excellent nanowires. Since their discovery, many advancements have been made, and nowadays, they can be obtained from the compression of several aromatic molecular crystals. However, it is often not clear why certain starting crystals give high-quality nanothreads while others do not or which are the best conditions for the synthesis in terms of pressure, temperature, compression rate, and reaction time. In other words, the mechanisms that allow their formation with respect to other byproducts are often unclear. This is an important piece of information that can be used for the design of a synthetic strategy for the production of functional materials with targeted characteristics, like conductivity and electro-optical properties, while preserving the mechanical ones. Here, we report an X-ray diffraction study in which we followed the transformation induced by the pressure of trans-azobenzene using polycrystalline samples compressed with and without a pressure-transmitting medium. With this approach, we were able to highlight the structural relations along the reactive path leading to double-core saturated carbon nanothreads. The features that we discovered could be common to all pseudo-stilbene crystals, a class of compounds isostructural to azobenzene and characterized by two phenyl rings connected by a variety of different linkers, thus representing excellent starting materials for the synthesis of functional nanothreads.

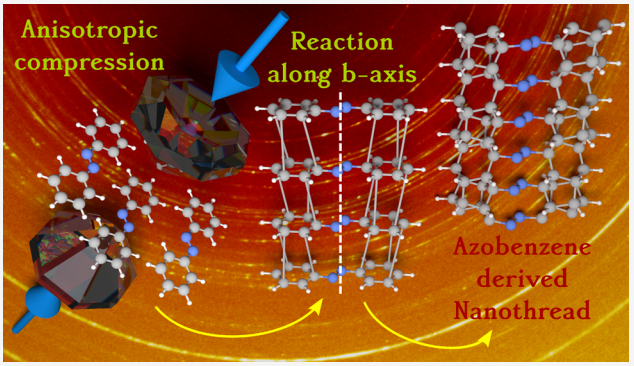

INTRODUCTION

The last decade was characterized by a revived interest for low-dimensional carbon materials that can be obtained by pressure-induced polymerization of aromatic hydrocarbons, with particular attention to a class of saturated carbon compounds having a structure resembling a unidimensional diamond-like wire.[1−4] These materials, generally called saturated carbon nanothreads, potentially possess extraordinary mechanical properties, being extremely flexible and resilient and preserving most of the tensile strength of the diamond, and are extremely attractive from a technological point of view.[5−8] These properties can be suitably tuned by controlling the thread length, the type and concentration of defects, and the presence of heteroatoms or functional groups, while preserving most of the mechanical properties.[5,6,9]

The existence of such materials was predicted since the early 2000s,[10−12] well before the first synthetic discovery that dates back to 2015 when bundles of saturated carbon nanothreads were found for the first time as a product of the high-pressure reaction of benzene crystals at 23 GPa and ambient temperature.[1] This was a very surprising finding because, so far, the high-pressure chemistry of benzene was thought to be well characterized.[13−16] Indeed, the thermodynamic and topochemical product of benzene that is obtained in many pressure and temperature conditions is an extended and amorphous hydrogenated carbon (a-C:H) compound that maintains a C/H ratio of 1/1. The mechanism of formation and the synthetic strategy to obtain carbon nanothreads instead of the extended compound were later well rationalized and identified in a crucial nontopochemical reaction step, induced by the uniaxial stress typically achieved in diamond anvil cell compression without any hydrostatic pressure-transmitting medium (PTM).[2,3]

Under this kind of compression, when a benzene crystallite in a polydispersed sample is rightly oriented with respect to the compression axis, the reactivity can be induced by the uniaxial stress, and the **b**−**c** stacks of benzene phase II are the best candidates for nanothread formation.[2] This reactivity can be induced even at a pressure lower than the one required for the (three-dimensional, 3D) bulk reaction leading to the extended

Received: May 5, 2021
Revised: July 8, 2021
Published: July 29, 2021

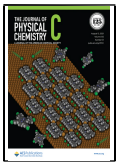

https://doi.org/10.1021/acs.jpcc.1c04003
J. Phys. Chem. C 2021, 125, 17174–17182

a-C:H, which is indeed partially avoided. The resulting product is hence formed by bundles of saturated carbon nanothreads packed in a pseudohexagonal two-dimensional (2D) lattice, with a lattice parameter of 6.5 Å corresponding to an interplanar distance of 5.6 Å, with the thread axis coincident with the applied stress direction.[1,2] As the topochemical reaction cannot be completely avoided, the formation of carbon nanothreads from benzene is never quantitative.

After the pioneering study on benzene, many theoretical studies have been done, showing the possibility of obtaining nanothreads from several aromatic, substituted aromatic, and heteroaromatic hydrocarbons, either six- or five-membered rings or polycyclics.[17−19] The possibility to introduce a certain concentration of a specific heteroatom or a functional group in the nanothread structure is of paramount importance to obtain materials with tailored chemical, optical, and electronic characteristics. From an experimental point of view, such nanothreads were obtained from the compression of pyridine,[4,20] thiophene,[21] furan,[22] aniline,[23] *para*-disubstituted benzenes,[24] polycyclic arene−perfluoroarene cocrystals,[25,26] and very recently azobenzene.[27] The combined effect of pressure and temperature has also been exploited, especially in the cases of aniline,[23,28] pyridine,[20] and azobenzene.[27] The temperature affects the amplitude of molecular motions due to lattice vibrations, with the beneficial effect of lowering the pressure threshold of the reaction and increasing its kinetics but also favoring the thermodynamic product, often in competition with the nanothread formation, unless they are the topochemical ones. From this point of view, aniline is a textbook example, as it is so far the only monomer that was found to quantitatively yield nanothread materials, even though in very drastic conditions (33 GPa, 550 K).[23] Nanothreads are indeed the topochemical product in this case because the crystal undergoes intrinsically anisotropic compression as its structure is ruled by strong and directional H-bonds among amino groups.[29] When the temperature is high enough to disrupt the H-bond network that is at the base of the anisotropic response of the crystal to pressure ($P < 20$ GPa, $T > 700$ K), the reaction mechanism changes and, as a consequence, the product is totally composed of an extended graphitic material.[28] In pyridine, there is a competition between the formation of an amorphous compound[30,31] and nanothreads[4] even at room temperature, in the high-pressure reaction ($P > 20$ GPa). In this case, while a mild heating little above 400 K enhances the nanothread yield up to 30%, improves the product quality, and lowers the pressure needed for the synthesis to 14 GPa, on further heating ($T > 650$K), the reaction turns quantitatively to the extended graphitic material already at 9 GPa.[20] An analogous effect is observed in trans-azobenzene.[27]

In some cases, the topology between the monomeric precursors in the original aromatic crystal and the nanothreads can be maintained, and then a careful selection of precursors that show (or develop in pressure) π-stacking along a certain crystallographic axis can be used to guide the reactivity toward a desired product structure, allowing a tailored bottom-up synthetic strategy.[25,26,32] In other words, the knowledge of the molecular arrangement in the crystal structure of a reactant and how it evolves with pressure up to the reaction threshold gives fundamental information on the possible reaction mechanism and allows prediction of the final product.[33] This information is fundamental to support a tailored synthesis, allowing the right choice of the starting materials, the design, and the optimization of the synthetic strategy, and eventually to obtain the desired functional material with high yield and high quality.

In a recent study, we showed that the compression of trans-azobenzene crystals, at ambient temperature over 20 GPa, leads to the formation of high-quality double-core nanothreads, where the azo group (−N═N−), which acts as a linker among the two cores, is preserved during the reaction and in the recovered material.[27] This result is of paramount importance because the azobenzene derivatives are the base of an entire family of dyes and their optical characteristics can be transferred to the corresponding carbon-saturated nanothreads if the azo group is maintained in the product. The photochemical and photophysical properties of the monomeric azobenzenes can be indeed finely tuned, for example, by changing the substituents in the phenyl rings.[34] Azobenzenes possess efficient photoisomerization capabilities, making them useful starting compounds for the realization of molecular devices,[35] functional materials,[36] and molecular photo-switches.[37−40]

The molecular arrangement in the crystal structure of azobenzene at ambient pressure[41,42] could be suggestive of a selective Dies−Alder [4 + 2] polymerization along the molecular stacks realized parallel to the **b** crystallographic axis, leading to the formation of nanothreads. However, at ambient conditions, the intermolecular distance is too long and the equivalent molecules are too tilted with respect to the **b** crystallographic axis to have any sort of π-interaction along the stack able to drive the reactivity along the **b** axis. The application of pressure could be very effective in developing such a kind of molecular interaction,[16,43] but this idea can be demonstrated only by the analysis of the pressure evolution of the structural parameters.

Here, we report the pressure evolution of the trans-azobenzene crystal parameters, obtained by means of synchrotron angle-dispersive X-ray diffraction at ambient temperatures up to the reaction threshold (∼20 GPa) using polycrystalline samples compressed with and without pressure-transmitting media. Precise topology relations between the reactant and the product are the outcome of this study, an important information that can be used in a tailored carbon nanothread synthesis.

METHODS

Crystalline trans-azobenzene (from Sigma-Aldrich with a purity >99%) was ground and loaded into a membrane diamond anvil cell (MDAC) equipped with type IIa synthetic diamonds from Almax easyLab Inc., together with some gold powder for pressure calibration, using the gold equation of state.[44] This choice was made to avoid any kind of laser light irradiation, like that necessary to excite the ruby fluorescence, because it can alter the sample and induce reactivity. All of the samples were laterally contained by steel gaskets, drilled to have an initial sample diameter of 150 μm and a thickness of about 50 μm. A first compression−decompression run was performed up to 12 GPa directed to the characterization of the equation of state of azobenzene, using N_2 as a pressure-transmitting medium, which was shown to be hydrostatic in this pressure range.[45] A second compression−decompression run was performed up to 24.5 GPa, without any pressure-transmitting medium to have an insight into the transformation of the reactant in double-core saturated carbon nanothreads bound together by azo-groups.[27]

https://doi.org/10.1021/acs.jpcc.1c04003
J. Phys. Chem. C 2021, 125, 17174−17182

Angle-dispersive synchrotron X-ray diffraction measurements were performed at the Xpress beamline at Elettra Sincrotrone Trieste (Italy) using a MAR345 image plate as a detector. The beam energy was set at 25 keV, corresponding to a wavelength of 0.49499 Å, with a beam diameter in the focus of about 80 μm (full width at half maximum, FWHM). An X-ray diffraction pattern was recorded every few kbar in both compression and decompression cycles. The detector was calibrated using a CeO_2 powder standard, and all of the data treatment and integration were performed using Dioptas 0.5.1 software,[46] while the integrated patterns were fit using Fityk 1.3.1 software[47] with a Voigt function for every diffraction peak. The intensity, angular position, and width of the reflections obtained in the hydrostatic compression were employed for indexing of powder diffraction patterns at each pressure step, by the Le Bail Monte Carlo method, using a modified version of McMaille 4.0 software[48] compiled to run under the Linux kernel.

Fourier transform infrared (FTIR) absorption spectra were recorded using a Bruker-IFS 120 HR spectrometer suitably modified for experiments in diamond anvil cells, with an instrumental resolution set to 1 cm^{-1}.[49] The ruby fluorescence was excited using <1 mW of a 532 nm laser line from a doubled Nd:YAG laser source, a power that was found to be unable to photoinduce azobenzene reactivity even for pressures higher than 10 GPa.

RESULTS AND DISCUSSION

Trans-azobenzene crystallizes in the monoclinic space group $P2_1/c$ with four molecules in the unit cell, each one lying on an inversion symmetry center of the lattice. There are two nonequivalent pairs of molecules, and half-molecule of each kind constitutes the asymmetric unit, one of them showing dynamic orientational disorder.[42,50] At ambient pressure, a good agreement of the cell parameters with the literature value is found.[41] The obtained values and the peak indexing obtained by the Le Bail method are reported in the Supporting Information (Tables S1 and S2). A comparison of representative integrated X-ray diffraction patterns and 2D detector images obtained under compression with and without pressure-transmitting medium of azobenzene powder is reported in Figure 1.

A selection of integrated patterns obtained for the hydrostatic compression−decompression cycle up to ∼12 GPa is reported in Figure 2. Every diffraction peak in the range $2 < 2\theta < 9°$ was fit with a Voigt function, and the maxima as a function of pressure are reported in the lower panel of Figure 3. The diffraction peaks of nitrogen (pressure-transmitting medium), appearing after solidification and marked with a star in Figure 2, do not overlap with the sample in this 2θ region, as they lie at $2\theta > 9°$. The intensity of the sample diffraction peaks diminishes with pressure, and the FWHM increases, resulting in a very difficult peak deconvolution for pressures higher than 12 GPa, a pressure very close to the hydrostatic limit of N_2 itself,[45] and for this reason, it was the final value of the compression run. In decompression, we had perfect reversibility of the peak maxima without any hysteresis and, after the complete download of the pressure, we recovered the initial crystalline quality of the powder, thus ruling out partial reactivity and amorphization. Even the line shape of the diffraction peaks is reversible in decompression, as to indicate that no stress is introduced in the powder, as expected for a hydrostatic compression. The absence of reactivity was

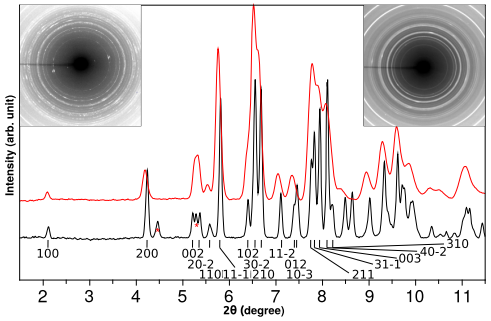

Figure 1. Integrated pattern of the azobenzene powder compressed without any hydrostatic pressure-transmitting medium at 1.9 GPa (red trace) compared to the one relative to a sample compressed with N_2 as a pressure-transmitting medium (PTM) at a similar pressure (black trace) and the relative 2D images: (left) with PTM and (right) without PTM. The peak assignment is limited to 2θ ∼8.5 because of the contribution from nitrogen above this angle. The reflections marked with an asterisk are not indexed for the azobenzene crystal structure.

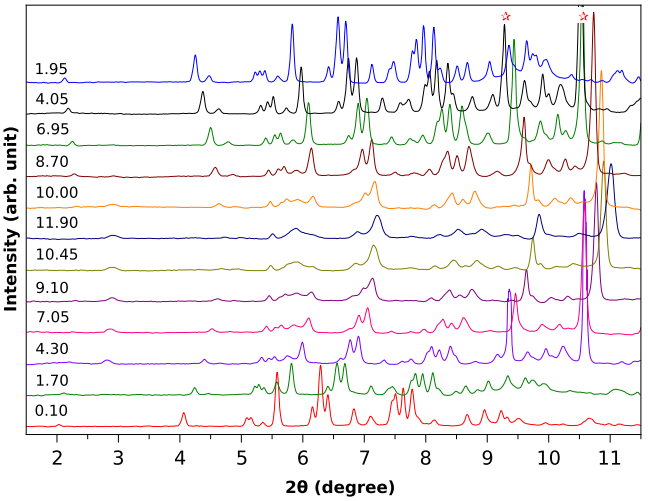

Figure 2. Selection of integrated patterns of azobenzene powder compressed with N_2 as pressure-transmitting medium reported as a function of pressure. For display convenience, a background is subtracted from every trace. The pressure values are in GPa units. The traces, from top to bottom, are relative to a compression up to ∼12 GPa and decompression to ambient pressure. The reflections marked with a star are relative to the solid N_2.

confirmed by FTIR spectroscopy, for a similar compression−decompression cycle up to the same pressure.

The cell parameters were obtained by Le Bail refinement deriving their starting values by the reflections at $2\theta < 6°$ that do not significantly overlap in all of the pressure ranges investigated (see Figure 2). Their behavior as a function of pressure (Figure 4) is the one expected for a soft molecular crystal up to ∼9 GPa. All of the three cell lengths reduce almost isotropically: **a** by about 12%, and **b** and **c** by about 10%, while the angle increases by less than 0.3°. Above this pressure and up to the maximum value we reached (12 GPa), the cell lengths stop to squeeze and the monoclinic angle β increases by ∼5.5° reaching 118.3°. In decompression, every crystal parameter is perfectly reversible without hysteresis. The error bars reported in Figure 4 represent the maximum variation of the parameter as obtained by composing the standard deviation from the Le Bail analysis with the major

https://doi.org/10.1021/acs.jpcc.1c04003
J. Phys. Chem. C 2021, 125, 17174−17182

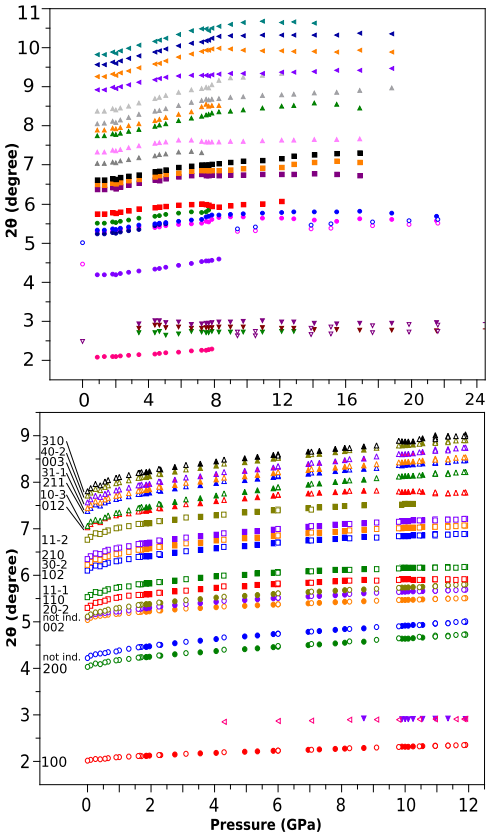

Figure 3. Peak maxima of reflections reported in 2θ as a function of pressure for the compression (full symbols) and decompression (empty symbols) of the azobenzene powder with N_2 as the pressure-transmitting medium (lower panel) and without any pressure-transmitting medium (upper panel). Miller indexes are also reported for the quasi-hydrostatic experiment. In the compression without the pressure-transmitting medium, the reflections relative to 100 and 200 disappear at about 8−9 GPa while a new set of reflections appears above 3 GPa at 2θ ∼3° and survive the compression−decompression cycle.

contribution deriving from the uncertainty in the peak assignment due to the overlap of reflections.

The volume of the azobenzene crystalline cell as a function of pressure was fit using the Rose−Vinet equation of state.[51] The values of the parameters and the fit are reported in Figure 5. We obtain a bulk modulus B_0 of 5.84 GPa and its pressure derivative B_0' of 9.49, values typical of a soft molecular crystal.[52] The better fit is performed excluding the volume values for pressures higher than 9.5 GPa, as these deviate from the equation of state valid for lower pressures. This observation in addition to the abrupt increase of the β angle of ∼5.5° is a clear indication of a phase transition happening at about 9.5 GPa, transition that is perfectly reversible in decompression without hysteresis. Other authors had hinted of a phase transition in this range of pressure, by performing Raman spectroscopy in nonhydrostatic compression.[53,54] In the same pressure range, the Davydov components of some infrared modes exchange intensity and some others undergo frequency discontinuities or change in the pressure slope, like that observed for the out-of-plane CH bending (γ_{CH}) or the mixed CC stretching and in-plane bending ($\delta_{CH} + \nu_{CC}$).[27]

The azobenzene powder was then pressurized at ∼25 GPa without any pressure-transmitting medium to induce the formation of carbon nanothreads[27] and have an insight into the reaction mechanism. We reached the pressure threshold for the irreversible reaction, and we observed how the Bragg peaks of the reactant transform into the ones characterizing the product. A selection of X-ray diffraction patterns is reported in Figure 6, while the peak maxima as a function of pressure, obtained by fitting each peak with a Voigt function, are reported in the upper panel of Figure 3. At about 3.5 GPa, a new set of reflections appears at 2θ ∼3°, a feature that also characterizes the nanothread product. These reflections cannot be indexed using the monoclinic structure of azobenzene and cannot be attributed to a product, as we know from FTIR spectroscopy that the crystal is chemically stable in this pressure range. The peaks can be more probably related to the activation of reflections like 001 or $10\bar{1}$, lying in this 2θ range but not supposed to have intensity in the monoclinic structure. This occurrence suggests the loss of the c-glide plane, which would imply symmetry lowering. Weak reflections at about $2\theta \simeq 3°$ also appeared in the quasi-hydrostatic experiment (see Figures 2 and 3) but at a considerably higher pressure (8.7 GPa). Since these peaks persist in the diffraction pattern of the nanothread, as observed in the experiment performed without pressure-transmitting medium, but cannot be related to a chemical reaction because of the perfect reversibility observed in the quasi-hydrostatic experiment, they are likely due to a rearrangement of the molecules in a geometry suggestive of that characterizing the nanothreads. All of these changes, as well as the progressive weakening of the 100 and 200 reflections above 3.5 GPa and their disappearance around 10 GPa, can be therefore ascribed to a phase transition. The abrupt pattern modification observed at about 7 GPa in the sample compressed without pressure-transmitting medium is instead not evident in the quasi-hydrostatic experiment. However, this can be due to the limited pressure reached in the latter experiment (11.9 GPa). In fact, all of the other changes described so far have been observed in both samples but with a higher pressure of about 5 GPa in the quasi-hydrostatic experiment. As can be seen in Figure 6, in the sample compressed without pressure-transmitting medium, all of the peaks lose intensity above 7 GPa till vanishing, except for the diffraction peaks that are present also in the nanothread product, like the reflection at 2θ ∼5.5°, deriving from the original 002 reflection of the azobenzene crystal. Despite the width of the Bragg peaks and the poor quality of the powder that is highly stressed in the nonhydrostatic compression, the cell parameters can be obtained by the Le Bail method, although affected by some error. The relevant reflections employed to this purpose are shown in the Supporting Information. The indexing of the unit cell parameters was indeed performed only in the monoclinic domain, neglecting every possible distortion of the α and γ angles from 90°, even though this kind of distortion is not unlikely because of the uniaxial stress.

In the range from 9.5 to 10.5 GPa, where the volume starts to deviate from the equation of state valid for lower pressures in the hydrostatic compression, we observe a clear sign of a phase transition, namely, an abrupt drop in the cell volume of ∼5.7%, which can be imputed almost totally to a ∼4.9% decrease of the **b** length and to a ∼5° increase of the monoclinic angle β. Above this pressure, and up to the highest pressure at which we still observe a reliable crystalline diffraction pattern (17−19 GPa), the **a** and **c** lengths and the β angle stay constant within the error, and the further reduction of the cell volume of about 9% can be then entirely

https://doi.org/10.1021/acs.jpcc.1c04003
J. Phys. Chem. C 2021, 125, 17174−17182

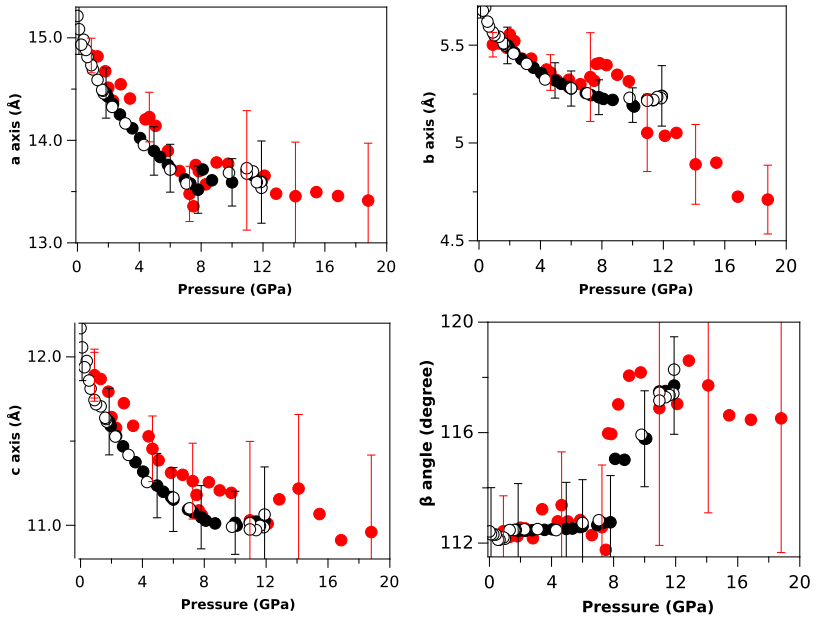

Figure 4. Cell parameters obtained by Le Bail refinement for the azobenzene powder: black dots are relative to compression (full black dots) and decompression (empty black dots) using N_2 as the pressure-transmitting medium, and red full dots are relative to the compression without any pressure-transmitting medium. The error bars, which for the sake of clarity are reported only for a reduced number of pressures, represent the maximum uncertainty in the parameter determination (see text).

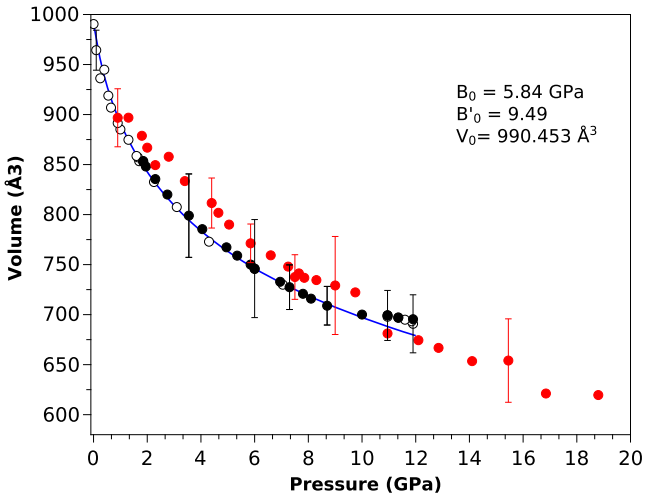

Figure 5. Volume of the azobenzene unit cell as a function of pressure obtained by Le Bail refinement for the powder with N_2 as pressure-transmitting medium in compression (full black dots) and decompression (empty dots) cycles, and the relative fit using the Rose−Vinet equation of state (blue line). The fit is performed in the range of pressures from ambient to 9.5 GPa. The bulk modulus (B_0) and its derivative with respect to pressure (B_0') obtained from the fit are also reported. The red dots are relative to the compression without any pressure-transmitting medium.

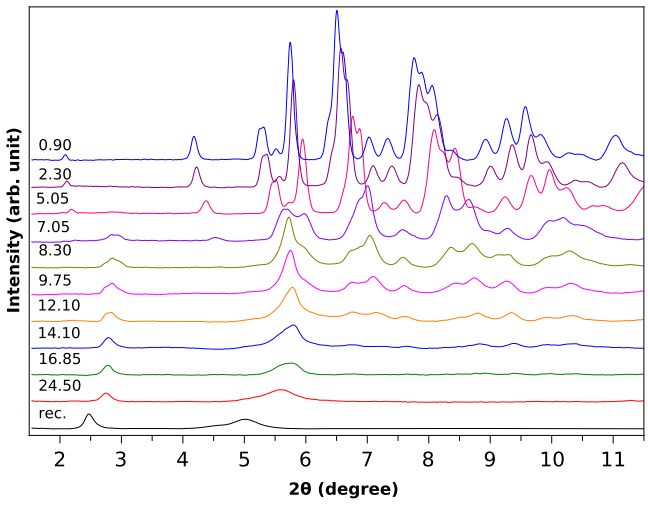

Figure 6. Selection of integrated patterns of azobenzene powder compressed without any hydrostatic pressure-transmitting medium as a function of pressure. The black trace is relative to the recovered material at ambient conditions taken outside of the DAC. For display convenience, a background is subtracted from every trace. The pressure values reported are in GPa units.

attributed to the **b** length, which decreases a further ∼7% in the pressure range of 11−19 GPa. This is a very important observation as the reactive approach for the formation of the carbon nanothreads was supposed to occur among equivalent molecules along the **b** axis, which indeed becomes the thread axis.[27] In the nanothread product, **ac** is the plane normal to the thread axis, where the distorted pseudohexagonal packing occurs. This packing can be viewed as a two-dimensional crystalline cell with the two main lengths of 13.05 and 6.45 Å, respectively, and an angle between them approaching the hexagonal one (120°), in which the electronic densities present along the azo-groups axis and the thread core axis, both parallel to the **b** crystallographic axis, act as scatterers.[27] This distorted pseudohexagonal structure has then the main Bragg diffraction peaks (100 and 001) lying, in the product obtained here, at 2θ values of 2.49 and 5.01°, respectively, and a third less intense peak at 2θ of 4.48° $(10\bar{1})$ as reported in Figure 6.

From FTIR measurements performed in the same conditions, aimed at the discovery of the pressure reaction threshold and the reaction kinetics, we know that azobenzene is chemically stable up to 20 GPa.[27] In addition, azobenzene needs to be kept at this pressure for several hours to have 20−

https://doi.org/10.1021/acs.jpcc.1c04003
J. Phys. Chem. C 2021, 125, 17174−17182

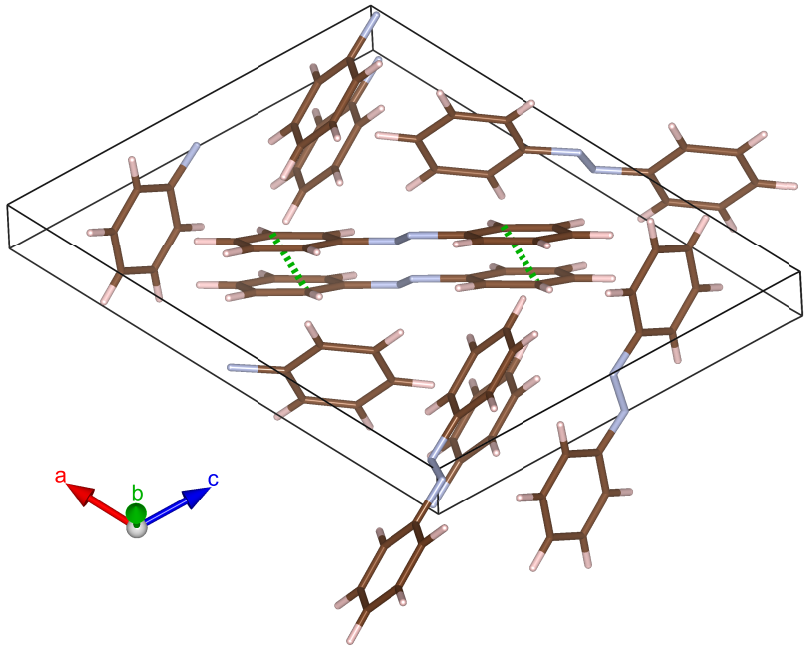

Figure 7. Structure of azobenzene at 19.5 GPa reconstructed considering the molecules are incompressible and using the relative atomic positions of the ambient pressure structure[41] and the cell parameters at this pressure, obtained in the compression without any pressure-transmitting medium (a = 13.40 Å, b = 4.65 Å, c = 10.95 Å, β = 118°). The shortest distances, reported in green, are between carbons belonging to neighboring equivalent molecules along the **b** axis, and they are 2.60 Å.

30% of monomer transformation. According to these results, we cannot assign any of the features observed up to 20 GPa to the chemical transformations of the monomer, being under the pressure threshold for the reaction. Therefore, the structural transformation induced by nonhydrostatic compression can be seen as a prereactive stage in which the equivalent molecules along the **b** crystallographic axis reorientate and start to interact along the stack by π-interactions as the **b** length shrinks and they come closer.

In Figure 7, we propose a reconstruction of the high-pressure structure of azobenzene at 19.5 GPa, very close to the reaction pressure threshold, obtained with the VESTA software.[55] The quality of the data relative to the compression without pressure-transmitting medium and the number of reflections surviving up to this pressure are not sufficient to perform a refinement of the atomic positions so that the atomic positions can only be presumed. The reconstruction is performed supposing that the azobenzene molecule is not distorted, the bond length and the relative orientation of the two nonequivalent molecules are unchanged, and barycenter positions in the crystalline cell are unaltered with increasing pressure. The only pressure effect taken into account is the modification of the cell parameters (lengths and angle). The parameters used for depicting the cell are therefore the ones obtained at 19.5 GPa in the nonhydrostatic compression (CIF file available as Supporting Information). Within this approximation, even if the reorientation of the molecules is not considered, the minimum C−C distance between neighboring molecules is realized among carbons belonging to molecules stacked along the **b** axis, and it is of 2.60 Å. This is a value at which a carbon−carbon σ-bond can be formed, aided by thermal motions[15,23,56] (details in the Supporting Information), making the approach along the **b** axis of equivalent molecules the most favorable to induce a reaction. Due to the same reasons, the reactivity proceeds preferentially along the stack rather than expanding in a tridimensional way, leading to the formation of double-core saturated carbon nanothreads. An explanation of the preferential compression along the **b** axis could be given supposing that the uniaxial stress is able to drive the π-electronic densities of the aromatic rings, aligned in a slipped parallel way along the **b** axis at ambient conditions, to interact over a certain pressure upon molecular reorientation, as in a prereactive stage. This occurrence can be the one driving the phase transition observed around 10 GPa, also in view of the abrupt negative slope increase of the pressure behavior of the **b** length over this pressure. This process finally leads to the one-dimensional (1D) reactive approach along the stack, which allows the formation of double-core saturated carbon nanothreads in a preferential way with respect to a 3D extended material. In this respect, the nanothreads can be seen as the topochemical product of azobenzene, while nonhydrostatically compressed.

CONCLUSIONS

Understanding the mechanism of a solid-state chemical reaction and the topological relations between the reactant and the product is of paramount importance in view of the design and optimization of a synthetic strategy to yield a high-quality functional material of the highest quantity. Without this knowledge, every synthesis is at risk of being tentative, and its recipe given more by chance than planning. In this work, we followed the evolution of the crystal structure of trans-azobenzene from ambient pressure up to the pressure of the spontaneous reaction, by means of powder X-ray diffraction using synchrotron light. By comparing the results of quasi-hydrostatic and nonhydrostatic experiments, we were able to understand how the product of the high-pressure reaction, i.e., double-core carbon-saturated nanothreads, forms. Using the Le Bail Monte Carlo method, we obtained the structural parameters of the azobenzene crystal as a function of pressure

https://doi.org/10.1021/acs.jpcc.1c04003
J. Phys. Chem. C 2021, 125, 17174−17182

by indexing up to 15−20 diffraction peaks for each pressure step.

In the presence of a quasi-hydrostatic pressure-transmitting medium, we have signs of a reversible phase transition at about 9.5 GPa, inducing a modification of the monoclinic angle β from 112.75 to 118.3° in few GPa, while the cell lengths stop to decrease, and as a consequence, the volume deviates from the equation of state valid for lower pressure, despite observing no discontinuity. Instead, in the compression without a pressure-transmitting medium that is intrinsically not hydrostatic, we observe an abrupt modification of the diffraction pattern already at ∼7 GPa, and consequently, an about 12% decrease of the cell volume that can be mainly imputed to the reduction of the **b** length of ∼5% and a modification of the β angle that approaches 120°, being clear signs of a phase transition. Above this pressure and up to the pressure of the spontaneous reaction, all of the cell parameters are almost unaffected with the notable exception of the **b** length that shortens a further ∼7% up to 19 GPa. This anisotropic compression of the crystalline cell induced by stress is at the base of the supposed reaction mechanism. The **b** axis is the one along which the nanothreads form, and it will become the nanothread axis itself, while the **ac** plane of the initial crystal will become the plane in which the distorted pseudohexagonal arrangement will be realized. At 20 GPa, pressure threshold of the spontaneous reaction, we have a minimum C−C equilibrium distance among the equivalent molecules aligned along the **b** axis of 2.60 Å, short enough to allow the formation of a C−C σ-bond, while aided by the thermal motions. As the other cell lengths do not shorten any more, there is a preferential axis for the reaction propagation, which is again the **b** axis, so that a tridimensional propagation of the reaction is avoided, and the product is hence the 1D saturated carbon nanothreads. Therefore, nanothreads are the topochemical high-pressure product of azobenzene, at least while nonhydrostatically compressed. A better definition of the reactive path and of the importance of the anisotropic compression could be provided by single-crystal diffraction studies using a hydrostatic compression medium up to the pressures of interest (about 20 GPa) such as helium or neon.

Azobenzene crystal is isostructural with stilbene and by extension with the pseudo-stilbenes. Due to the structural similarity and the similar kind of weak interactions that characterize these molecular crystals, they have the possibility to form inclusion or mixed crystals in any reciprocal ratio.[41,57] The findings that we reported here could be common to the whole class of pseudo-stilbenes, and all of them could be excellent starting materials for the carbon nanothread synthesis. In this view, the chemical, optical, and electronic characteristics of the resulting products could be finely tuned by suitably changing the ratio and the composition of azobenzene/pseudo-stilbenes in the starting mixed crystal for a tailored synthesis of double-core saturated carbon nanothreads.

■ ASSOCIATED CONTENT

Supporting Information

The Supporting Information is available free of charge at https://pubs.acs.org/doi/10.1021/acs.jpcc.1c04003.

Raman spectra of azobenzene crystal in the phonon region; calculation of thermal displacement amplitudes in the azobenzene crystal at the reaction threshold; ambient pressure values of the azobenzene cell parameters; diffraction peak indexing obtained by the Le Bail method; and selected patterns, and relative indexing, of the nonhydrostatically compressed powder covering all of the pressure ranges studied (PDF)

Crystallographic data (CIF)

■ AUTHOR INFORMATION

Corresponding Author

Samuele Fanetti − *European Laboratory for Nonlinear Spectroscopy (LENS), 50019 Sesto Fiorentino, FI, Italy; Consiglio Nazionale delle Ricerche—Istituto di Chimica dei Composti OrganoMetallici, 50019 Sesto Fiorentino, FI, Italy;* orcid.org/0000-0002-5688-6272; Phone: +39 055 457 2536; Email: fanetti@lens.unifi.it

Authors

Sebastiano Romi − *European Laboratory for Nonlinear Spectroscopy (LENS), 50019 Sesto Fiorentino, FI, Italy;* orcid.org/0000-0002-9553-7788

Frederico Alabarse − *Elettra Sincrotrone Trieste S.C.p.A, 34149 Basovizza, TS, Italy;* orcid.org/0000-0002-7375-3666

Roberto Bini − *European Laboratory for Nonlinear Spectroscopy (LENS), 50019 Sesto Fiorentino, FI, Italy; Consiglio Nazionale delle Ricerche—Istituto di Chimica dei Composti OrganoMetallici, 50019 Sesto Fiorentino, FI, Italy; Dipartimento di Chimica "Ugo Schiff", Università di Firenze, 50019 Sesto Fiorentino, FI, Italy;* orcid.org/0000-0002-6746-696X

Complete contact information is available at: https://pubs.acs.org/10.1021/acs.jpcc.1c04003

Notes

The authors declare no competing financial interest.

■ ACKNOWLEDGMENTS

The authors thank the European Laboratory for Nonlinear Spectroscopy (LENS) for hosting part of the research, and the Fondazione Cassa di Risparmio di Firenze for the strong support. The research has been supported by the following grant: Fondazione Cassa di Risparmio di Firenze under the project "Utilizzo dell'anisotropia strutturale nella sintesi di nanofili di carbonio diamond-like ad alta pressione". The authors acknowledge Elettra Sincrotrone Trieste for providing access to its synchrotron radiation facilities and for financial support under the proposal number 20200230.

■ REFERENCES

(1) Fitzgibbons, T. C.; Guthrie, M.; Xu, E.; Crespi, V. H.; Davidowski, S. K.; Cody, G. D.; Alem, N.; Badding, J. V. Benzene-derived carbon nanothreads. *Nat. Mater.* **2015**, *14*, 43−47.

(2) Li, X.; Baldini, M.; Wang, T.; Chen, B.; Xu, E.-s.; Vermilyea, B.; Crespi, V. H.; Hoffmann, R.; Molaison, J. J.; Tulk, C. A.; et al. Mechanochemical Synthesis of Carbon Nanothread Single Crystals. *J. Am. Chem. Soc.* **2017**, *139*, 16343−16349.

(3) Chen, B.; Hoffmann, R.; Ashcroft, N. W.; Badding, J.; Xu, E.; Crespi, V. Linearly Polymerized Benzene Arrays As Intermediates, Tracing Pathways to Carbon Nanothreads. *J. Am. Chem. Soc.* **2015**, *137*, 14373−14386.

(4) Li, X.; Wang, T.; Duan, P.; Baldini, M.; Huang, H.-T.; Chen, B.; Juhl, S. J.; Koeplinger, D.; Crespi, V. H.; Schmidt-Rohr, K.; et al. Carbon Nitride Nanothread Crystals Derived from Pyridine. *J. Am. Chem. Soc.* **2018**, *140*, 4969−4972.

(5) Roman, R. E.; Kwan, K.; Cranford, S. W. Mechanical Properties and Defect Sensitivity of Diamond Nanothreads. *Nano Lett.* **2015**, *15*, 1585−1590.
(6) Zhan, H.; Zhang, G.; Tan, V. B. C.; Cheng, Y.; Bell, J. M.; Zhang, Y.-W.; Gu, Y. From brittle to ductile: a structure dependent ductility of diamond nanothread. *Nanoscale* **2016**, *8*, 11177−11184.
(7) Zhan, H.; Zhang, G.; Bell, J. M.; Tan, V. B. C.; Gu, Y. High density mechanical energy storage with carbon nanothread bundle. *Nat. Commun.* **2020**, *11*, No. 1905.
(8) Zhan, H.; Zhang, G.; Zhuang, X.; Timon, R.; Gu, Y. Low interfacial thermal resistance between crossed ultra-thin carbon nanothreads. *Carbon* **2020**, *165*, 216−224.
(9) Zheng, Z.; Zhan, H.; Nie, Y.; Xu, X.; Gu, Y. Role of Nitrogen on the Mechanical Properties of the Novel Carbon Nitride Nanothreads. *J. Phys. Chem. C* **2019**, *123*, 28977−28984.
(10) Barua, S. R.; Quanz, H.; Olbrich, M.; Schreiner, P. R.; Trauner, D.; Allen, W. D. Polytwistane. *Chem. - Eur. J.* **2014**, *20*, 1638−1645.
(11) Wen, X.-D.; Hoffmann, R.; Ashcroft, N. W. Benzene under High Pressure: a Story of Molecular Crystals Transforming to Saturated Networks, with a Possible Intermediate Metallic Phase. *J. Am. Chem. Soc.* **2011**, *133*, 9023−9035.
(12) Stojkovic, D.; Zhang, P.; Crespi, V. H. Smallest Nanotube: Breaking the Symmetry of sp^3 Bonds in Tubular Geometries. *Phys. Rev. Lett.* **2001**, *87*, No. 125502.
(13) Ciabini, L.; Santoro, M.; Bini, R.; Schettino, V. High pressure reactivity of solid benzene probed by infrared spectroscopy. *J. Chem. Phys.* **2002**, *116*, 2928−2935.
(14) Ciabini, L.; Gorelli, F.; Santoro, M.; Bini, R.; Schettino, V.; Mezouar, M. High-pressure and high-temperature equation of state and phase diagram of solid benzene. *Phys. Rev. B: Condens. Matter Mater. Phys.* **2005**, *72*, No. 094108.
(15) Ciabini, L.; Santoro, M.; Gorelli, F.; Bini, R.; Schettino, V.; Raugei, S. Triggering dynamics of the high-pressure benzene amorphization. *Nat. Mater.* **2007**, *6*, 39−43.
(16) Citroni, M.; Bini, R.; Foggi, P.; Schettino, V. Role of excited electronic states in the high-pressure amorphization of benzene. *Proc. Natl. Acad. Sci. U.S.A.* **2008**, *105*, 7658−7663.
(17) Demingos, P. G.; Muniz, A. R. Carbon nanothreads from polycyclic aromatic hydrocarbon molecules. *Carbon* **2018**, *140*, 644−652.
(18) Silveira, J. F. R. V.; Muniz, A. R. Functionalized diamond nanothreads from benzene derivatives. *Phys. Chem. Chem. Phys.* **2017**, *19*, 7132−7137.
(19) Demingos, P. G.; Balzaretti, N. M.; Muniz, A. R. First-principles study of carbon nanothreads derived from five-membered heterocyclic rings: thiophene, furan and pyrrole. *Phys. Chem. Chem. Phys.* **2021**, *23*, 2055−2062.
(20) Fanetti, S.; Santoro, M.; Alabarse, F.; Enrico, B.; Bini, R. Modulating the H-bond strength by varying the temperature for the high pressure synthesis of nitrogen rich carbon nanothreads. *Nanoscale* **2020**, *12*, 5233−5242.
(21) Biswas, A.; Ward, M. D.; Wang, T.; Zhu, L.; Huang, H.-T.; Badding, J. V.; Crespi, V. H.; Strobel, T. A. Evidence for Orientational Order in Nanothreads Derived from Thiophene. *J. Phys. Chem. Lett.* **2019**, *10*, 7164−7171.
(22) Huss, S.; Wu, S.; Chen, B.; Wang, T.; Gerthoffer, M. C.; Ryan, D. J.; Smith, S. E.; Crespi, V. H.; Badding, J. V.; Elacqua, E. Scalable Synthesis of Crystalline One-Dimensional Carbon Nanothreads through Modest-Pressure Polymerization of Furan. *ACS Nano* **2021**, *15*, 4134−4143.
(23) Nobrega, M. M.; Teixeira-Neto, E.; Cairns, A. B.; Temperini, M. L. A.; Bini, R. One-dimensional diamondoid polyaniline-like nanothreads from compressed crystal aniline. *Chem. Sci.* **2018**, *9*, 254−260.
(24) Tang, W. S.; Strobel, T. A. Evidence for Functionalized Carbon Nanothreads from π-Stacked, para-Disubstituted Benzenes. *J. Phys. Chem. C* **2020**, *124*, 25062−25070.
(25) Ward, M. D.; Tang, W. S.; Zhu, L.; Popov, D.; Cody, G. D.; Strobel, T. A. Controlled Single-Crystalline Polymerization of $C_{10}H_8$·$C_{10}F_8$ under Pressure. *Macromolecules* **2019**, *52*, 7557−7563.
(26) Friedrich, A.; Collings, I. E.; Dziubek, K. F.; Fanetti, S.; Radacki, K.; Ruiz-Fuertes, J.; Pellicer-Porres, J.; Hanfland, M.; Sieh, D.; Bini, R.; et al. Pressure-Induced Polymerization of Polycyclic Arene-Perfluoroarene Cocrystals: Single Crystal X-ray Diffraction Studies, Reaction Kinetics, and Design of Columnar Hydrofluorocarbons. *J. Am. Chem. Soc.* **2020**, *142*, 18907−18923.
(27) Romi, S.; Fanetti, S.; Alabarse, F.; Mio, A. M.; Bini, R. Synthesis of double core chromophore-functionalized nanothreads by compressing azobenzene in a Diamond Anvil Cell. *Chem. Sci.* **2021**, *12*, 7048−7057.
(28) Fanetti, S.; Nobrega, M. M.; Teixeira-Neto, E.; Temperini, M. L. A.; Bini, R. Effect of Structural Anisotropy in High-Pressure Reaction of Aniline. *J. Phys. Chem. C* **2018**, *122*, 29158−29164.
(29) Fanetti, S.; Citroni, M.; Dziubek, K.; Nobrega, M. M.; Bini, R. The role of H-bond in the high-pressure chemistry of model molecules. *J. Phys.: Condens. Matter* **2018**, *30*, No. 094001.
(30) Fanetti, S.; Citroni, M.; Bini, R. Structure and reactivity of pyridine crystal under pressure. *J. Chem. Phys.* **2011**, *134*, No. 204504.
(31) Zhuravlev, K. K.; Traikov, K.; Dong, Z.; Xie, S.; Song, Y.; Liu, Z. Raman and infrared spectroscopy of pyridine under high pressure. *Phys. Rev. B* **2010**, *82*, No. 064116.
(32) Gerthoffer, M. C.; Wu, S.; Chen, B.; Wang, T.; Huss, S.; Oburn, S. M.; Crespi, V. H.; Badding, J. V.; Elacqua, E. Sacrificial' supramolecular assembly and pressure-induced polymerization: toward sequence-defined functionalized nanothreads. *Chem. Sci.* **2020**, *11*, 11419−11424.
(33) Lauher, J. W.; Fowler, F. W.; Goroff, N. S. Single-Crystal-to-Single-Crystal Topochemical Polymerizations by Design. *Acc. Chem. Res.* **2008**, *41*, 1215−1229.
(34) Bandara, H. M. D.; Burdette, S. C. Photoisomerization in different classes of azobenzene. *Chem. Soc. Rev.* **2012**, *41*, 1809−1825.
(35) Singleton, T. A.; Ramsay, K. S.; Barsan, M. M.; Butler, I. S.; Barrett, C. J. Azobenzene Photoisomerization under High External Pressures: Testing the Strength of a Light-Activated Molecular Muscle. *J. Phys. Chem. B* **2012**, *116*, 9860−9865.
(36) Wagner-Wysiecka, E.; Łukasik, N.; Biernat, J. F.; Luboch, E. Azo group(s) in selected macrocyclic compounds. *J. Inclusion Phenom. Macrocyclic Chem.* **2018**, *90*, 189−257.
(37) Bushuyev, O. S.; Corkery, T. C.; Barrett, C. J.; Friščić, T. Photo-mechanical azobenzene cocrystals and in situ X-ray diffraction monitoring of their optically-induced crystal-to-crystal isomerisation. *Chem. Sci.* **2014**, *5*, 3158−3164.
(38) Bléger, D.; Hecht, S. Visible-Light-Activated Molecular Switches. *Angew. Chem., Int. Ed.* **2015**, *54*, 11338−11349.
(39) Crespi, S.; Simeth, N. A.; König, B. Heteroaryl azo dyes as molecular photoswitches. *Nat. Rev. Chem.* **2019**, *3*, 133−146.
(40) Dong, M.; Babalhavaeji, A.; Samanta, S.; Beharry, A. A.; Woolley, G. A. Red-Shifting Azobenzene Photoswitches for in Vivo Use. *Acc. Chem. Res.* **2015**, *48*, 2662−2670.
(41) Bouwstra, J. A.; Schouten, A.; Kroon, J. Structural Studies of the System trans-Stilbene/trans-Azobenzene. III. The Structures of Three Mixed Crystals of trans-Azobenzene/trans-Stilbene; Determinations by X-ray and Neutron Diffraction. *Acta Crystallogr., Sect. C: Cryst. Struct. Commun.* **1985**, *41*, 420−426.
(42) Brown, C. J. A refinement of the crystal structure of azobenzene. *Acta Crystallogr.* **1966**, *21*, 146−152.
(43) Fanetti, S.; Citroni, M.; Bini, R. Pressure-induced fluorescence of pyridine. *J. Phys. Chem. B* **2011**, *115*, 12051−12058.
(44) Heinz, D. L.; Jeanloz, R. The equation of state of the gold calibration standard. *J. Appl. Phys.* **1984**, *55*, 885−893.
(45) Klotz, S.; Chervin, J.-C.; Munsch, P.; Marchand, G. L. Hydrostatic limits of 11 pressure transmitting media. *J. Phys. D: Appl. Phys.* **2009**, *42*, No. 075413.
(46) Prescher, C.; Prakapenka, V. B. DIOPTAS: a program for reduction of two-dimensional X-ray diffraction data and data exploration. *High Pressure Res.* **2015**, *35*, 223−230.

https://doi.org/10.1021/acs.jpcc.1c04003
J. Phys. Chem. C 2021, 125, 17174−17182

(47) Wojdyr, M. *ityk*: a general-purpose peak fitting program. *J. Appl. Crystallogr.* **2010**, *43*, 1126−1128.
(48) Le Bail, A. Monte Carlo indexing with McMaille. *Powder Diffr.* **2004**, *19*, 249−254.
(49) Bini, R.; Ballerini, R.; Pratesi, G.; Jodl, H. J. Experimental setup for Fourier transform infrared spectroscopy studies in condensed matter at high pressure and low temperatures. *Rev. Sci. Instrum.* **1997**, *68*, 3154−3160.
(50) Harada, J.; Ogawa, K. X-ray Diffraction Analysis of Non-equilibrium States in Crystals: Observation of an Unstable Conformer in Flash-Cooled Crystals. *J. Am. Chem. Soc.* **2004**, *126*, 3539−3544.
(51) Vinet, P.; Smith, J.; Ferrante, J.; Rose, J. Temperature effects on the universal equation of state of solids. *Phys. Rev. B* **1987**, *35*, 1945−1953.
(52) Bini, R.; Schettino, V. *Materials Under Extreme Conditions*; Imperial College Press, 2014.
(53) Dong, Z.; Seemann, N. M.; Lu, N.; Song, Y. Effects of High Pressure on Azobenzene and Hydrazobenzene Probed by Raman Spectroscopy. *J. Phys. Chem. B* **2011**, *115*, 14912−14918.
(54) Li, A.; Bi, C.; Xu, S.; Cui, H.; Xu, W. Structural change of trans-azobenzene crystal and powder under high pressure. *J. Mol. Struct.* **2020**, *1206*, No. 127745.
(55) Momma, K.; Izumi, F. VESTA: a three-dimensional visualization system for electronic and structural analysis. *J. Appl. Crystallogr.* **2008**, *41*, 653−658.
(56) Citroni, M.; Fanetti, S.; Bazzicalupi, C.; Dziubek, K.; Pagliai, M.; Nobrega, M. M.; Mezouar, M.; Bini, R. Structural and Electronic Competing Mechanisms in the Formation of Amorphous Carbon Nitride by Compressing s-Triazine. *J. Phys. Chem. C* **2015**, *119*, 28560−28569.
(57) Bouwstra, J. A.; Schouten, A.; Kroon, J. Structural studies of the system *trans*-azobenzene/*trans*-stilbene. I. A reinvestigation of the disorder in the crystal structure of *trans*-azobenzene, $C_{12}H_{10}N_2$. *Acta Crystallogr., Sect. C: Cryst. Struct. Commun.* **1983**, *39*, 1121−1123.

https://doi.org/10.1021/acs.jpcc.1c04003
J. Phys. Chem. C 2021, 125, 17174−17182